JCI The Journal of Clinical Investigation

Sex-dependent compensatory mechanisms preserve blood pressure homeostasis in prostacyclin receptor deficient mice

Soon Y. Tang, … , Gregory R. Grant, Garret A. FitzGerald

J Clin Invest. 2021. https://doi.org/10.1172/JCI136310.

Research In-Press Preview **Vascular biology**

Inhibitors of mPges-1 are in the early phase of clinical development. Deletion of mPges-1 in mice confers analgesia, restrains atherogenesis and fails to accelerate thrombogenesis, while suppressing PGE2, but increasing biosynthesis of PGI2. In $Ldlr^{-/-}$ mice, this last effect represents the dominant mechanism by which mPges-1 deletion restrains thrombogenesis, while suppression of PGE2 accounts for its anti-atherogenic effect. However, the impact of mPges-1 depletion on BP in this setting remains unknown. Here, mPges-1 depletion significantly increased the BP response to salt loading in male $Ldlr^{-/-}$ mice, whereas, despite the direct vasodilator properties of PGI2, Ipr deletion suppressed it. Furthermore, combined deletion of the Ipr abrogated the exaggerated BP response in male mPges-$1^{-/-}$ mice. Interestingly, these unexpected BP phenotypes were not observed in female mice fed a high salt diet. This is attributable to the protective effect of estrogen in $Ldlr^{-/-}$ mice and in $Ipr^{-/-}$ /$Ldlr^{-/-}$ mice. Thus, estrogen compensates for a deficiency in PGI2 to maintain BP homeostasis in response to high salt in hyperlipidemic female mice. In males, by contrast, augmented formation of ANP plays a similar compensatory role, restraining hypertension and oxidant stress in the setting of Ipr depletion. Hyperlipidemic males on a high salt diet might be at risk of a hypertensive response to mPGES-1 inhibitors.

Sex-dependent compensatory mechanisms preserve blood pressure homeostasis in prostacyclin receptor deficient mice

[1]Soon Yew Tang, PhD; [1]Hu Meng, PhD, [1]Seán T. Anderson, PhD; [1,2]Dimitra Sarantopoulou, MSc; [1]Soumita Ghosh, PhD; [1]Nicholas F. Lahens, PhD; [1]Katherine N. Theken, [1]Emanuela Ricciotti, PhD; [1]Elizabeth J. Hennessy, PhD; [3]Vincent Tu, PhD; [3]Kyle Bittinger, PhD; [1]Aalim Weiljie, PhD; [1,4]Gregory R. Grant, PhD; [1]*Garret A. FitzGerald, MD

[1]From the Institute for Translational Medicine and Therapeutics, Perelman School of Medicine, Department of Systems Pharmacology and Translational Therapeutics, [2]Current address at National Institute on Aging, National Institutes of Health, 21224. [3]Division of Gastroenterology, Hepatology, and Nutrition, Children's Hospital of Philadelphia, Philadelphia, PA 19104-5127. [4]Department of Genetics, University of Pennsylvania, Philadelphia, Pennsylvania, 19104-5127.

*Address for correspondence: Garret A. FitzGerald, Institute for Translational Medicine and Therapeutics, Perelman School of Medicine, 10-110 Smilow Center for Translational Research, 3400 Civic Center Blvd, Bldg 421, University of Pennsylvania, Philadelphia, PA 19104-5158. Fax: 215-573-9135. Tel: 215-898-1184. Email: garret@upenn.edu

Subject code: Vascular Disease

Abstract

Inhibitors of mPges-1 are in the early phase of clinical development. Deletion of mPges-1 in mice confers analgesia, restrains atherogenesis and fails to accelerate thrombogenesis, while suppressing PGE_2, but increasing biosynthesis of PGI_2. In $Ldlr^{-/-}$ mice, this last effect represents the dominant mechanism by which mPges-1 deletion restrains thrombogenesis, while suppression of PGE_2 accounts for its anti-atherogenic effect. However, the impact of mPges-1 depletion on BP in this setting remains unknown. Here, mPges-1 depletion significantly increased the BP response to salt loading in male $Ldlr^{-/-}$ mice, whereas, despite the direct vasodilator properties of PGI_2, Ipr deletion suppressed it. Furthermore, combined deletion of the Ipr abrogated the exaggerated BP response in male mPges-$1^{-/-}$ mice. Interestingly, these unexpected BP phenotypes were not observed in female mice fed a high salt diet. This is attributable to the protective effect of estrogen in $Ldlr^{-/-}$ mice and in $Ipr^{-/-}$ /$Ldlr^{-/-}$ mice. Thus, estrogen compensates for a deficiency in PGI_2 to maintain BP homeostasis in response to high salt in hyperlipidemic female mice. In males, by contrast, augmented formation of ANP plays a similar compensatory role, restraining hypertension and oxidant stress in the setting of Ipr depletion. Hyperlipidemic males on a high salt diet might be at risk of a hypertensive response to mPGES-1 inhibitors.

Key words: Ipr, mPges-1, ANP, hyperlipidemia, hypertension, indoles, sexual dimorphism

Introduction

Both the adverse cardiovascular events associated with non-steroidal anti-inflammatory drugs (NSAIDs) and the opioid crisis have prompted interest in developing new analgesics (1-4). Several clinical trials have shown that the incidence and severity of hypertension from NSAID use is quite variable in humans (5-8). Inhibitors of the microsomal PGE synthase -1 (mPGES-1), an enzyme involved in the biosynthesis of prostaglandin (PG) E_2, are in early clinical development as potential non-addictive analgesics devoid of the cardiovascular hazards attributable to inhibition of cyclooxygenase-2 (COX-2) by NSAIDs.

Deletion of mPges-1 has a mild adverse cardiovascular profile in normolipidemic mice (3) and we have reported that rediversion of the mPGES-1 substrate prostaglandin (PG)H_2 to prostacyclin (PGI_2) synthase, augmenting PGI_2, attenuates thrombogenesis in hyperlipidemic mice (9). This is a point of distinction from Cox-2 depletion or inhibition that suppresses synthesis of this endogenous platelet inhibitor and predisposes mice to thrombogenic stimuli (3).

Sexual dimorphism in blood pressure (BP) homeostasis is at least partly explained by the endocrine system. For example, systolic blood pressure (SBP) is higher in boys from 13 years on compared with girls of the same age (10) and the hypertensive response to salt loading is more pronounced in apparently healthy males compared to premenopausal females at different ages (11). Similarly, in genetically and experimentally predisposed rodent models, hypertension develops more slowly in female than in male mice (12, 13). Deletion of prostaglandin E_2 receptor, Epr1, reduced BP in male but not female mice (14). Besides, BP homeostasis is also closely linked to the immune system, inflammation and composition of gut microbiota (15-17). Both in human and rodent studies, high salt diets have been shown to increase BP while

decreasing α- and β-diversity of the microbiome (18). Amongst others, *Lactobacillus* species displayed a negative association with BP responses (19).

Here, the BP response to a high salt diet (HSD) is augmented in hyperlipidemic mice lacking the low-density lipoprotein receptor (Ldlr). Both PGE_2 and PGI_2 may act as direct vasodilators so we assumed that exaggeration of this response in mPges-1 mice was attributable to suppression of PGE_2, despite their augmented formation of PGI_2. To our surprise, deletion of the Ipr attenuated the hypertensive response to mPges-1 deletion. Furthermore, this was observed in male, but not female mice. Mechanistically, we found that Ipr deletion results in a release of the vasodilator, atrial natriuretic peptide (ANP) (20, 21) and attenuation of the oxidant stress that characterizes hyperlipidemia (22) in male mice. This results in abrogation of the hypertensive response to salt. In females, by contrast, these responses were not observed, while in ovariectomized mice estrogen attenuated salt-evoked hypertension in both $Ldlr^{-/-}$ and $Ipr^{-/-}/Ldlr^{-/-}$ mice but not in mPges-$1^{-/-}/Ldlr^{-/-}$ mice. HSD significantly reduced the abundance of *Lactobacillus* only in male mice, coinciding with a reduction in their fecal product indole-3-lactic acid. Reduction of this metabolomics restraint on inflammation and oxidative stress may have contributed to the sexually dimorphic, exaggerated salt induced hypertension that we observed.

Results

Deletion of the Ipr in mPges-1-deficient hyperlipidemic mice abrogates salt-evoked hypertension

Hyperlipidemic mice ($Ldlr^{-/-}$) were used in the current study to simulate more closely the atherosclerosis likely extant in elderly patients targeted for analgesia with mPGES-1 inhibitors. As shown in Supplemental Figures 1A-1D, despite feeding a chow diet, plasma cholesterol and/ or triglyceride levels of $Ldlr^{-/-}$, Ipr- and mPges-1-deficient $Ldlr^{-/-}$ mice were significantly elevated.

Male $Ldlr^{-/-}$ mice fed a HSD showed a time-dependent elevation of SBP in the active (night) period (Figure 1A- 1B). The SBP was significantly elevated in week 2 compared with baseline during the active phase. Deletion of mPges-1 significantly increased further the salt-evoked BP response. By contrast, deletion of the Ipr unexpectedly restrained the hypertensive response to the HSD in both $Ldlr^{-/-}$ and mice also lacking mPges-1. At baseline, male mice lacking both mPges-1 and Ldlr had elevated BP compared to the other genotypes (Figure 1). Thereafter the attenuating effects of Ipr deletion became apparent: SBPs of $Ldlr^{-/-}$, mPges-$1^{-/-}$/$Ldlr^{-/-}$ and $Ipr^{-/-}$ /mPges-$1^{-/-}$/$Ldlr^{-/-}$ mice were significantly elevated compared with $Ipr^{-/-}$/$Ldlr^{-/-}$ mice one week and/ or two weeks after feeding them the HSD. Similar differences in diastolic blood pressure (DBP) responses were observed in all mutants and their littermate controls fed a HSD in the active and resting periods (Figure 1C- 1D). DBP in $Ldlr^{-/-}$ mice was significantly elevated at week 2 compared with baseline during the active phase. Compared with $Ipr^{-/-}$/$Ldlr^{-/-}$ mice, the DBPs of $Ldlr^{-/-}$, mPges-$1^{-/-}$/$Ldlr^{-/-}$ and $Ipr^{-/-}$/mPges-$1^{-/-}$/$Ldlr^{-/-}$ mice were significantly elevated at baseline, one week and/ or two weeks after HSD feeding. However, these HSD evoked BP responses were not observed in female hyperlipidemic mice (Supplemental Figure 2A- 2D). In addition, weight gain, urinary output/ fluid intake ratio and urinary sodium levels did not appear to explain the sex differences in BP responses to the salt loading in our mice (Supplemental Figure 3A- 3C). We were not able to measure accurately food intake in the current study because the HSD was very hygroscopic.

Detailed statistical analyses of the interactions among genotypes, treatment (week) and phases for both sexes are described in supplemental Figure 4.

Impact of Ipr and mPges-1 deletion on prostaglandin biosynthesis in male hyperlipidemic mice on a high salt diet

Two weeks of HSD feeding suppressed PGE_2 but increased PGI_2 biosynthesis in male $Ldlr^{-/-}$ mice, as reflected in their urinary PGEM (7-hydroxy-5, 11-diketotetranorprostane-1, 16-dioic acid) and PGIM (2, 3-dinor 6-keto $PGF_{1\alpha}$) metabolites, respectively (Figure 2A- 2B). Overall (Figure 2), deletion of mPges-1 in the hyperlipidemic mice ($mPges\text{-}1^{-/-}/Ldlr^{-/-}$) suppressed PGE_2 and augmented formation of PGI_2, thromboxane $(Tx)B_2$ and PGD_2 as expected consequent to substrate rediversion. These changes were more pronounced on the HSD. Finally, deletion of the Ipr resulted in a reactionary increase in biosynthesis of PGI_2, but also of TxB_2 and PGD_2, again apparent on an HSD.

Detailed statistical analyses of the interactions among urinary prostaglandin metabolites, genotypes and treatment (week) are described in supplemental Figure 5.

Pharmacological inhibition of the human mPGES-1 enzyme elevates systolic blood pressure in hyperlipidemic male mice

To confirm the hypertensive phenotype of global $mPges\text{-}1^{-/-}/Ldlr^{-/-}$ mice, an mPGES-1 inhibitor (MF970, 10 mg/Kg BW) was administered concomitantly with a high fat diet (HFD) for 39 weeks in humanized mPGES-1 $Ldlr^{-/-}$ male mice. As shown in Supplemental Figure 6, inhibition of mPGES-1 suppressed urinary PGEM (A) and elevated SBP response (B) as compared to control with the HFD alone.

A HSD activates atrial natriuretic peptide synthesis and release in Ipr-deficient mice

The unexpected suppression of the salt-evoked elevation of BP by Ipr deletion prompted us to compare gene expression profiles in the renal medullae of male $Ldlr^{-/-}$ and $Ipr^{-/-}/Ldlr^{-/-}$ mice by high throughput RNA sequencing. We identified 2719 DEGs), with a log fold change ranging from 2.64 to -3.83 between $Ldlr^{-/-}$ and $Ipr^{-/-}/Ldlr^{-/-}$ mice at a false discovery rate (FDR) cutoff of 0.12. One thousand ninety-seven of these 2719 DEGs were upregulated and 1622 were downregulated in the renal medulla of $Ipr^{-/-}/Ldlr^{-/-}$ mice compared to $Ldlr^{-/-}$ mice. Ingenuity Pathway analysis (IPA) was used to assess changes in biological pathways associated with gene expression (Table 1) and the pathways most enriched with DEGs included eukaryotic initiation factor (eIF2), eIF4/ p70S6K signaling, mitochondrial dysfunction and oxidative phosphorylation. Sixty-three of the 76 identified genes in the eIF2 pathway were downregulated in the $Ipr^{-/-}/Ldlr^{-/-}$ mice, mostly members of the 60s and 40s ribosomal subunits involved in RNA binding (Figure 3A and Supplemental Table 1). Forty-five of 47 genes related to mitochondrial dysfunction and oxidative phosphorylation were downregulated in the $Ipr^{-/-}/Ldlr^{-/-}$ mice (Figure 3A and Supplemental Table 1). Most of these genes are components of mitochondrial complexes I to V, which are involved in electron transport and ATP synthesis. We validated three of the genes (Downregulated; Atp5e- a subunit of mitochondrial ATP synthase. Upregulated; Cat and Sod2- antioxidant enzymes) in the mitochondrial dysfunction and oxidative phosphorylation pathways by RT-qPCR (Supplemental Figure 7A- 7B). In addition, the RNA-Seq data are consistent with activation of the atrial natriuretic peptide (ANP) pathway. Expression of neprilysin (Mme) that degrades natriuretic peptides was elevated in $Ipr^{-/-}/Ldlr^{-/-}$ mice compared with $Ldlr^{-/-}$ mice (Figure 3B). We confirmed by RT-qPCR analyses that mRNA levels of corin (ANP-converting enzyme) and ANP, but not brain natriuretic peptide (BNP), were significantly increased in whole heart lysate in $Ipr^{-/-}/Ldlr^{-/-}$ mice (Figure 3C- 3E). Moreover, renal medullary expression of Npr1, a

receptor of ANP, was significantly increased (Figure 3F). Consistent with the gene expression data, urinary ANP levels were also elevated in $Ipr^{-/-}/Ldlr^{-/-}$ mice compared with $Ldlr^{-/-}$ mice after two weeks on the HSD (Figure 4A- 4B). We did not observe a significant difference in creatinine levels in the urine samples between $Ldlr^{-/-}$ and $Ipr^{-/-}/Ldlr^{-/-}$ mutants (Supplemental Figure 3D). Thus, elevated urinary ANP levels were not likely to be confounded by differences in fluid intake. Consistent with the role of PGI_2 in restraining oxidative stress in atherosclerotic vasculature (23) and in salt-induced hypertension (24, 25) and the elevation of PGI_2 biosynthesis on the HSD (Figure 2), excretion of a major urinary F_2-isoprostane (F_2iP), an index of lipid peroxidation, was not significantly elevated in $Ldlr^{-/-}$ mice after 2 weeks on a HSD (Figure 4C and 4D). However, rather than increase with Ipr deletion, F_2iP excretion, just like BP, unexpectedly fell, consistent with the changes in mitochondrial dysfunction and oxidative phosphorylation genes observed in the renal medulla of $Ipr^{-/-}/Ldlr^{-/-}$ mice (mostly downregulated in the $Ipr^{-/-}/Ldlr^{-/-}$ mice) (Figure 4D). The reduction in urinary F_2iP and elevated ANP levels consequent to Ipr deletion in the $Ldlr^{-/-}$ mice was abrogated by treatment with the ANP receptor antagonist, A71915 (26-28) (Figure 4E and 4F). This is consistent with evidence that ANP is both a vasodilator and a restraint on oxidative stress (27, 29).

The hypotensive phenotype of $Ipr^{-/-}/Ldlr^{-/-}$ mice was not associated with gross morphological changes in the kidney (Supplemental Figure 8) or the vasculature (Supplemental Figure 9) based on H&E staining. In male mice, deletion of the Ipr has no significant effect on urinary total nitrate + nitrite (Supplemental Figure 10A) or plasma renin levels (Supplemental Figure 10B) compared with $Ldlr^{-/-}$ mice.

In contrast to the males, expression of corin, ANP and BNP mRNAs in whole heart and the three mitochondrial dysfunction and oxidative phosphorylation genes (Atp5e, Cat and Sod2) in the

renal medulla were not significantly altered between female $Ldlr^{-/-}$ and $Ipr^{-/-}/Ldlr^{-/-}$ mice fed the HSD for two weeks (Supplemental Figure 11A- 11E). Urinary F_2iP did not differ significantly in female $Ipr^{-/-}/Ldlr^{-/-}$ mice compared to $Ldlr^{-/-}$ mice at baseline (Supplemental Figure 12A) or after two weeks on a HSD (Supplemental Figure 12B). However, combined deletion of Ipr and ANP receptor blockade in females significantly increased urinary F_2iPs (Supplemental Figure 12C), while deletion of the Ipr significantly reduced baseline urinary ANP (Supplemental Figure 12D). This difference was abolished after two weeks on the HSD (Supplemental Figure 12E); blockade of the ANP receptor did not alter ANP levels between $Ldlr^{-/-}$ and $Ipr^{-/-}/Ldlr^{-/-}$ mice (Supplemental Figure 12F). These results were consistent with the failure of genotype to influence significantly the HSD evoked BP response in female mice (Supplemental Figure 2).

Sex-dependent immunological responses induced by a HSD

Given our findings on sex differences in BP responses, we were interested to compare the transcriptomic profiles of atria from female and male $Ldlr^{-/-}$ and $Ipr^{-/-}/Ldlr^{-/-}$ mice fed a HSD for two weeks. We identified 177 DEGs (136 are unique to female, 11 are unique to male, 30 are common between female and male), with a log fold change ranging from 5.00 to -3.84 at a FDR cutoff of 0.4 (Supplemental Figure 13A). In females, 110 of the 166 DEGs were downregulated and 56 were upregulated in $Ipr^{-/-}/Ldlr^{-/-}$ mice compared with $Ldlr^{-/-}$ mice. In male mice, 17 of the 41 DEGs were downregulated and 24 were upregulated in $Ipr^{-/-}/Ldlr^{-/-}$ mice. IPA revealed pathways most enriched with DEGs including antigen presentation pathway, B cell development and T cell receptor signaling (Supplemental Figure 13B and Table 2). In female mice, DEGs associated with the classical or nonclassical major histocompatibility complex (MHC) class I molecules including C5ar2, Rfx5, H2-M3, H2-Q5, H2-Q6, C5ar1, H2-Aa, H2-Q7,H2-T22, H2-

DMb1, Nlrc5 and H2-T10 were downregulated in Ipr$^{-/-}$/Ldlr$^{-/-}$ mice compared with Ldlr$^{-/-}$ mice, and only C5ar2 was downregulated in male Ipr$^{-/-}$/Ldlr$^{-/-}$ mice. We validated H2-M3 DEG by RT-qPCR (Supplemental Figure 13C). The functional output analysis predicted inflammatory responses and chronic inflammatory disorders as downstream pathways likely to be affected by the DEGs. However, there was not a strong degree of consistency in the directions of the DEGs (Supplemental Figure 13D and Supplemental Table 2). Both T helper 17 cells and T-regulatory cells have been shown to modulate BP responses in hypertensive mouse models. Depletion of Ipr significantly increased plasma levels of IL-17A (Supplemental Figure 13E) and cardiac mRNA levels of IL-17 receptor A (IL-17ra, Supplemental Figure 13F) and transcription factor of T-regulatory cells (Foxp3, Supplemental Figure 13G) in male Ldlr$^{-/-}$ mice.

An atrial natriuretic peptide antagonist rescues hypotension in Ipr-deficient hyperlipidemic mice on a high salt diet

Due to the physiological constraint of implanting both radio telemetry probes and mini-pumps in mice for monitoring BP and delivering the ANP antagonist during HSD feeding, we decided to use the tail-cuff system for the former while delivering the antagonist by mini-pumps. Despite being less sensitive, BP data collected with the tail-cuff system correlate with those from radio telemetry (Figure 5A- 5B).

Inhibition of the endogenous ANP signaling pathway with the antagonist, A71915 (27), attenuated the hypotensive response to Ipr deletion in the HSD fed male Ipr$^{-/-}$/Ldlr$^{-/-}$ mice during both the night and day periods (Figure 5A- 5B and Supplemental Figure 14- sham-saline). Consistent with this, no significant differences in atrial and ventricular corin, ANP and BNP mRNA levels were observed between male Ldlr$^{-/-}$ and Ipr$^{-/-}$/Ldlr$^{-/-}$ mice treated with the

antagonist (Supplemental Figure 15A- 15F). Similarly, the difference in expression of the Npr1 receptor for ANP in renal medulla (Supplemental Figure 15G), and three of the genes (Atp5e, Cat and Sod2) in the mitochondrial dysfunction and oxidative phosphorylation pathways (Supplemental Figure 16A- 16C) were abolished by antagonist administration. Administration of A71915 did not alter plasma creatinine levels between male $Ldlr^{-/-}$ and $Ipr^{-/-}/Ldlr^{-/-}$ mice (Supplemental Figure 15H). As expected in female mice, no differences in SBP or plasma creatinine were observed between $Ldlr^{-/-}$ and $Ipr^{-/-}/Ldlr^{-/-}$ mice fed a HSD for two weeks in conjunction with ANP receptor blockade (Supplemental Figure 17A- 17B).

Detailed statistical analyses of the interactions between BP, genotypes and treatment (week) in A71915 study in male mice are described in Supplemental Figure 18.

Estrogen protects female hyperlipidemic mice from salt-evoked hypertension

To address the female BP phenotypes, we performed the HSD experiment using ovariectomized mice (OVX). HSD significantly increased BP responses in OVX $Ldlr^{-/-}$ mice in week 2 compared with baseline during both the active and resting periods (Figure5C- 5D). Deletion of Ipr augmented the SBP responses and supplementation with estradiol (E2) significantly restrained these responses (Figure 5C-5D). Similar differences in DBP responses were observed in $Ldlr^{-/-}$ and Ipr-deficient $Ldlr^{-/-}$ mice (Figure 5E- 5F). As expected, no significant differences in BP responses were detected among the sham-operated mice fed an HSD for 2 weeks (Supplemental Figure 19A-19D).

Detailed statistical analyses of the interactions among genotypes ($Ldlr^{-/-}$ and $Ipr^{-/-}/Ldlr^{-/-}$ mice), E2 and treatment (week) of OVX mice are described in Supplemental Figure 20.

HSD alters gut microbiota composition in a sex-dependent manner

To study the impact of sex and Ipr depletion on the gut microbiome in our mouse model of salt-evoked hypertension, we subjected female and male $Ldlr^{-/-}$ and $Ipr^{-/-}$/ $Ldlr^{-/-}$ mice to a HSD for 2 weeks. Fecal samples at day 0 and day 14 were analyzed by 16S rRNA marker gene sequencing. The taxonomic identities of prominent Amplicon Sequence Variants (ASVs) are presented in the heat map in Supplemental Figure 21 (mean relative abundance among all parameters of > 0.5%). A comparison of the microbiome on day 0 vs day 14 revealed that HSD was associated with decreased α-diversity (Faith's PD) in female $Ipr^{-/-}$/$Ldlr^{-/-}$ mice (p= 0.034, Supplemental Figure 22A). The bacterial community, as analyzed by unweighted and weighted UniFrac, was different between days 0 and 14 in both sexes and genotypes (Figure 6A- 6B). At the genus level, the relative abundance of *Lactobacillus* decreased in male $Ldlr^{-/-}$ (p= $1.2x10^{-3}$, Figure 6C) and $Ipr^{-/-}$/ $Ldlr^{-/-}$ mice (p= $2.5x10^{-4}$, Figure 6C) mice but not in female mice. Several taxa were changed over time in both sexes and genotypes: *Bacteroidales S24-7*and *Staphylococcus* increased in relative abundance, while *Mucispirillum* and *Helicobacter* decreased. *Corynebacterium* was detected only in male mice and increased after HSD feeding (Supplemental Figure 22B).

When we examined the effect of sex on the gut microbiota after HSD feeding, we found that the α-diversity between female and male mice was not different (Supplemental Figure 22C), but we did observe differences in β-diversity (unweighted UniFrac) at day 0 in $Ldlr^{-/-}$ mice (p= 0.01) and at day 14 in $Ipr^{-/-}$/$Ldlr^{-/-}$ mice (p= 0.01, Supplemental Figure 22D). At day 14, the relative abundance of *Lactobacillus* was decreased (p= 0.03) in male $Ipr^{-/-}$/ $Ldlr^{-/-}$ mice compared with females (Supplemental Figure 22E). To gain further insight into the types of Lactobacillus observed, we aligned representative sequences from our experiment to species type strains and assigned species where our sequences matched to within 2 bp. Thus, we observed a decrease in

sequences consistent with *Lactobacillus intestinalis* (p= 1.6x10^{-4}) in male Ldlr$^{-/-}$ mice relative to female mice (Supplemental Figure 22F). We found no differences in α-diversity or β-diversity between Ldlr$^{-/-}$ and Ipr$^{-/-}$/ Ldlr$^{-/-}$ mice at day 0 or day 14 in both female and male mice (Supplemental Figure 23A-23B).

HSD alters microbiota-derived fecal indole metabolites and short-chain fatty acids

As HSD significantly reduced the abundance of *Lactobacillus* in male mice compared to female mice regardless of genotype, we were interested to measure microbiota-derived fecal indole metabolites and short-chain fatty acids (SCFAs) by LC-MS/MS and H^1-NMR, respectively. Since Ipr deletion did not alter both α- and β-diversity of gut microbiota in both female and male mice, we combined both genotypes in our analyses to determine the effect of HSD on fecal metabolites. As shown in Figure 6C, HSD significantly increased fecal indole-3- acetic acid (IAA), whereas indole-3-propionic acid (IPA) was decreased in both female and male mice. However, indole-3-lactic acid (ILA) was significantly decreased only in male mice. Consistent with the decreased abundance of *Lactobacillus*, fecal lactic acid contents were significantly reduced in both female and male mice after a HSD feeding (Supplemental Figure 24A-24B). A similar pattern was observed for fecal butyric acid, but only in male mice was a significant reduction attained. Fecal acetic and propionic acids were unaltered in both sexes.

HSD differentially alters plasma metabolites in female and male mice

The impacts of Ipr deletion and sex differences on metabolic activity were analyzed further using plasma samples by UPLC-MS/MS in a semi-targeted approach. Orthogonal partial least squares-discriminant analysis (OPLS-DA) of genotype and sex revealed a distinct separation between

female Ldlr$^{-/-}$ (red spheres) and male Ldlr$^{-/-}$ (green spheres) mice after 2 weeks on a HSD (Supplemental Figure 25A). OPLS-DA loadings' plot identified indoxyl sulfate, trimethylamine oxide, propylene glycol and methyl adenosine metabolites were significantly higher in female Ldlr$^{-/-}$ mice (Supplemental Figure 25B). Metabolites such as orotate, deoxyuridine, cytidine, carnitine etc on the right side of the plot (P1>0) were significantly higher in the male Ldlr$^{-/-}$ mice. MetaboAnalyst pathway analysis revealed several metabolic differences between female and male mice, including phenylalanine, tyrosine, tryptophan and pyrimidine (Supplemental Figure 25C). Notably, "tryptophan metabolite" was one of the most impacted metabolic pathways between female and male Ldlr$^{-/-}$ mice after feeding a HSD for two weeks. To corroborate with our microbiota-induced changes in indole metabolites, we focused on the tryptophan/ indole pathway. Indeed, consistent with the reduction in abundance of *Lactobacillus*, plasma indoxyl sulfate/ tryptophan (Figure 6E) was significantly decreased in male Ldlr$^{-/-}$ mice compared with female Ldlr$^{-/-}$ mice, whereas tryptophan and kynurenine levels were not altered between female and male mice regardless of their genotypes (Supplemental Figure 25D).

Discussion

NSAIDs represent an alternative to opioid analgesics but themselves confer a cardiovascular hazard attributable to suppression of COX-2 derived cardioprotective prostaglandins, especially PGI_2 (30). PGI_2 restrains platelet activation and is a vasodilator; deletion of its Ipr receptor predisposes normolipidemic mice to thrombogenic and hypertensive stimuli (3, 31, 32). Given the importance of PGE_2 as a mediator of pain and inflammation, interest has focused on the development of inhibitors of mPGES-1, the enzyme downstream of COX-2 that is the dominant source of PGE_2 biosynthesis (1, 2).

In normolipidemic mice, deletion of mPges-1, unlike deletion of Cox-2 or the Ipr, has a bland adverse cardiovascular profile; it does not promote thrombogenesis and it restrains atherogenesis (3, 33). This reflects rediversion of the PGH_2 substrate of mPGES-1 to other PG synthases, most relevantly to augment PGI_2 biosynthesis (34). Depending on genetic background, it may leave basal and evoked BP responses unchanged or modestly increased. On a hyperlipidemic background, increased PGI_2 limited thrombogenesis while suppression of PGE_2 accounted for restraint of atherogenesis when mPges-1 was deleted (9). Inhibition of mPGES-1 in humans also augments biosynthesis of PGI_2 coincident with suppression of PGE_2 (35).

Initially, we wished to examine the impact of mPges-1 deletion on BP in hyperlipidemic mice. Both PGE_2 and PGI_2 may act as vasodilators and deletion of their Epr2 and Ipr receptors predisposed normolipidemic mice to HSD induced elevations of BP (31, 32, 36). Here, we found that mPges-1 deletion predisposed hyperlipidemic male, but not female mice, to the pressor response to HSD, consistent with the role of PGE_2 in fluid volume and BP homeostasis (37). Moreover, chronic exposure to a pharmacological inhibitor (MF970) specifically targeting human mPGES-1 resulted in elevated SBP in hyperlipidemic mice on a HFD. These observations raise the possibility that despite results in healthy volunteers (28), inhibition of mPGES-1 in male patients with hyperlipidemia may predispose them to an exaggerated BP response to a HSD.

To investigate whether the augmented PGI_2 biosynthesis resulting from mPges-1 deletion might be buffering the hypertensive phenotype we utilized mice lacking the Ipr. We were surprised to find that BP responses to salt loading in male, but not female mice, was attenuated (rather than exacerbated) in $Ipr^{-/-}$/mPges-$1^{-/-}$ mice. Deletion of the Ipr resulted in a compensatory increase in biosynthesis of PGI_2 consequent to salt loading. However, given the absence of its receptor, this

would be unlikely to influence BP homeostasis directly. Rather, we found activation of another compensatory mechanism, increased formation of the vasodilator ANP. Antagonism of its Npr1 receptor was sufficient to rescue the hypotensive response to a HSD in Ipr depleted mice. The ANP promoter contains cyclic (c)AMP response element binding sites. Normally, of the Ipr by PGI_2 results in activation of protein kinase A (PKA) and elevation of intracellular cAMP (38). In the absence of its cognate receptor, the augmented PGI_2 in male Ipr $^{-/-}$ mice may activate other PKA linked receptors, such as Epr2, Epr4 and Dpr1. Indeed, HSD also increased biosynthesis of PGD_2 that acting through Dpr1 may augment this effect. Thus, altered patterns of eicosanoid formation in Ipr mice on a HSD may act via this mechanism to effect a compensatory elevation of ANP.

Hyperlipidemia in Ldlr$^{-/-}$ mice is associated with oxidative stress, reflected by increased generation of F_2iPs, biomarkers of lipid peroxidation (22). Both PGI_2 and ANP can act to restrain oxidative stress which itself may contribute to elevation of BP in response to a HSD (23, 39, 40). Here we found that despite augmented biosynthesis of PGI_2, urinary F_2iP was depressed in Ipr$^{-/-}$/Ldlr$^{-/-}$ mice compared to mice lacking the Ldlr alone. To address the possibility that this reflected the compensatory augmentation of ANP, we treated the mice with an ANP receptor antagonist and found that like the hypotensive phenotype, it rescued the suppression of F_2iP in the Ipr$^{-/-}$/Ldlr$^{-/-}$ mice. Pathway enrichment analyses of RNA-sequencing data also reflected a shift in redox balance in the renal medulla of the Ipr$^{-/-}$/Ldlr$^{-/-}$ mice. Some 45 genes related to mitochondrial dysfunction and oxidative phosphorylation are downregulated while genes encoding antioxidant enzymes, including mitochondrial superoxide dismutase (SOD2) and catalase, are upregulated. Again, ANP antagonism rescued this signature, adding evidence

consistent with an antioxidant effect of functional relevance. Although the ANP/ Npr1 pathway plays an important role in regulating blood volume and pressure (41, 42), we failed to observe comparative diuresis or natriuresis in the $Ipr^{-/-}/Ldlr^{-/-}$ mice. Similarly, urinary total nitrate/ nitrite and plasma renin levels were unaltered in the $Ipr^{-/-}/Ldlr^{-/-}$ mice compared to $Ldlr^{-/-}$ controls. These differences in the BP response to a HSD and the attendant changes in gene expression and activation of the ANP pathway were observed only in male mice. There is prior evidence for the influence of sex and genetic background on disruption of the prostaglandin pathways. For example, we have shown that deletion of the Ipr accelerates atherogenesis particularly in female mice due to the importance of PGI_2 as a mediator of estrogen receptor dependent cardioprotection (23).

Estrogen increases vasodilation partly by binding to its receptors in vascular endothelial and smooth muscle cells (SMC) of the vasculature (43). Consistent with the findings that estradiol activates PGI_2 biosynthesis in rat aortas (44), rat aortic SMC (45) and human endothelial cells (46), ovariectomy augmented the hypertensive response to a HSD in $Ldlr^{-/-}$ and Ipr-deficient $Ldlr^{-/-}$ mice. Estradiol replacement restrained the elevation in BP in the female ovariectomized mice consistent with our observation of sexual dimorphism in the response to Ipr deletion and the BP response to a HSD.

There is increasing evidence suggesting that T cells mediate inflammatory processes associated with hypertension in humans (16, 47, 48). Rodent models of hypertension have also been associated with upregulation of pathogenic Th17 cells and downregulation of protective T-regulatory cells (16, 49-51). Here, deletion of the Ipr increased serum IL-17A and cardiac IL-17ra mRNA levels in male $Ldlr^{-/-}$ mice consistent with PGI_2 restraining salt-induced oxidative stress and differentiation of naïve T cells to pathogenic Th17 cells. We speculate that the

increase in cardiac Foxp3 mRNA levels, a transcription factor of T-regulatory cells may reflect a response to counteract the increase in Th17 cells. In an airway allergen-sensitive mouse model, PGI_2 signaling promoted differentiation of suppressive T regulatory cells via Fxop3 transcription factor to restrain immunoglobulin-like transcript 3 (ILT3) driven allergic inflammation (52). Others have shown that female rats with increased T-regulatory cells were protected from DOCA-salt-evoked hypertension compared with male rats (47). Here deletion of the IPr also perturbed the immune profile of atrial transcripts in a sexually dimorphic manner. For example, "antigen presentation pathway", "B cell development" and "T cell receptor signaling" were enriched in hyperlipidemic females by deletion of the IPr. Additionally, DEGs associated with the classical or nonclassical MHC class I molecules were down regulated in females compared to males.

Although deletion of Ipr failed to alter HSD-induced changes in the composition of gut microbiota in $Ldlr^{-/-}$ mice, HSD had a sexually dimorphic impact on the gut microbiome. Consistent with other studies (47, 53), we observed a significant decrease in the abundance of *Lactobacillus* in male, but not female mice fed a HSD for 2 weeks. *Lactobacillus* is able to metabolize tryptophan to indole metabolites, including IAA, IPA and ILA, which act via binding to AhR to modulate innate and adaptive immunity responses (54). For example, ILA-producing *Lactobacillus murinus* was reported to restrain HSD-induced inflammatory T_H17 cells in the spleen, small intestine and colon and rescue salt- sensitive hypertension in FVB/N male mice (47). Importantly, ILA induces differentiation of $CD4^+$ T helper cells into double-positive intraepithelial lymphocytes via binding to the AhR. This effect was abrogated in AhR deficient T helper cells (55). Correspondingly, indoxyl sulfate/ tryptophan was reduced in plasma in male mice consistent with a differential impact on tryptophan metabolism contributing to the

sensitivity of BP to a HSD in male $Ldlr^{-/-}$ mice. Previous clinical studies have demonstrated that fecal microbiota-derived indole metabolites may activate AhR to modulate different immune responses in health and disease (56, 57).

In summary, we report distinct sex dependent compensatory mechanisms to preserve BP homeostasis in response to disruption of the receptor for the direct vasodilator, PGI_2 (Figure 7). In males, deletion of the Ipr restrains salt-evoked hypertension via activation of the ANP/Npr1 pathway reducing the oxidative stress characteristic of hyperlipidemia. It remains to be seen if this compensatory response wanes under conditions of chronic intake of a HSD, as might be most clinically relevant. In female mice, estrogen restrains the BP responses of both $Ldlr^{-/-}$ and $Ipr^{-/-}/Ldlr^{-/-}$ mice to salt-evoked hypertension. Irrespective of the impact of IPr deletion, depletion of *Lactobacillus* in the gut results in perturbation of tryptophan metabolism that may exaggerate the hypertensive response of male mice to a HSD.

Finally, our findings with mPges-1 deletion or pharmacological inhibition of the enzyme in mice suggest that hyperlipidemic male patients, consuming a high salt diet, may be susceptible to hypertension when taking mPGES-1 inhibitors.

Methods

All reagents used were purchased from Sigma-Aldrich (St. Louis, MO) unless otherwise stated. Detailed descriptions of the animal models and experimental methods are provided in the Supplemental Methods.

Statistics

All animals were the same age and on the same $LdIr^{-/-}$ background (C57BL/6). Where conclusions involve multiple factors, two-, three- and four-way ANOVA with repeated measures

was used to investigate changes in mean scores at multiple time points and differences in mean scores under multiple conditions. The residuals are normally distributed as required by ANOVA. The degrees of freedom were corrected using Greenhouse-Geisser estimates of sphericity. ANOVA tests were repeated on multiple restricted models to investigate combinations of factors' effects. Post-hoc analysis was performed by pairwise *t*-tests, with Bonferroni correction unless otherwise stated. A significance threshold of 0.05 was used for all tests. Significance of greater than 0.01 is indicated by double-asterisks on the graphs and significance greater than 0.001is indicated by triple-asterisks unless otherwise stated. Sample sizes were based on power analysis from estimates of the variability of the measurements and the desire to detect a minimal 10% difference in the variables assessed with $\alpha = 0.05$ and the power $(1-\beta) = 0.8$.

Study approval

All animals in this study were housed according to the guidelines of the Institutional Animal Care and Use Committee (IACUC) of the University of Pennsylvania. All experimental protocols were approved by IACUC (protocol #804754).

Author contributions

SYT, HM, STA, DS, SG, NFL, KNT, VT and GRG contributed to acquiring and analyzing data. SYT, ER, EH, KB, AW and GAF contributed to data interpretation. SYT and GAF conceived of the study and are responsible for the experimental design and manuscript preparation.

Acknowledgements

We gratefully acknowledge the advice of Dr. Matthew Palmer (Hospital of the University of Pennsylvania) on mouse kidney morphology and technical support of Weili Yan, Helen Zhou and Wenxuan Li-Feng.

Sources of Funding

Supported by a grant (HL062250) from the National Institutes of Health. GAF is the McNeil Professor of Translational Medicine and Therapeutics.

Disclosures

None

Table 1. Top Canonical Pathways Predicted by Ingenuity Pathway Analysis for the 2719 Differentially Expressed Genes in Kidney Medulla between Male Ldlr$^{-/-}$ and Ipr$^{-/-}$/Ldlr$^{-/-}$ Mice on a HSD.

Canonical Pathway	***P*-value**	**Overlap**
eIF2 Signaling	8.27E-21	76/194
Oxidative Phosphorylation	2.62E-17	47/99
Mitochondrial Dysfunction	8.26E-16	60/159
Regulation of eIF4 and p70S6K Signaling	4.06E-08	47/164

76 of the 194 genes associated with eIF2 signaling pathway were differentially expressed in Ipr$^{-/-}$ /Ldlr$^{-/-}$ vs Ldlr$^{-/-}$.

Table 2. Top Canonical Pathways Predicted by Ingenuity Pathway Analysis for the 177 Differentially Expressed Genes in Atria between Female $Ldlr^{-/-}$ and $Ipr^{-/-}/Ldlr^{-/-}$ Mice on a HSD.

Canonical Pathway	***P*-value**	**Overlap**	**Molecules Represented**
Antigen Presentation	2.57E-08	6/27	H2-Q2, H2-DMb1, H2-Aa, H2-M3, Nlrc5, Psmb9
B Cell Development	2.45E-05	4/25	H2-Q2, H2-DMb1, H2-Aa, Ptprc
T Cell Receptor Signaling	2.75E-05	9/148	Grap2, H2-T10, H2-T22, H2-Q2, H2-DMb1, H2-Aa, H2-M3, Prkcq, Ptprc

6 of the 27 genes associated with antigen presentation signaling pathway were differentially expressed in $Ipr^{-/-}/Ldlr^{-/-}$ vs $Ldlr^{-/-}$.

Figure

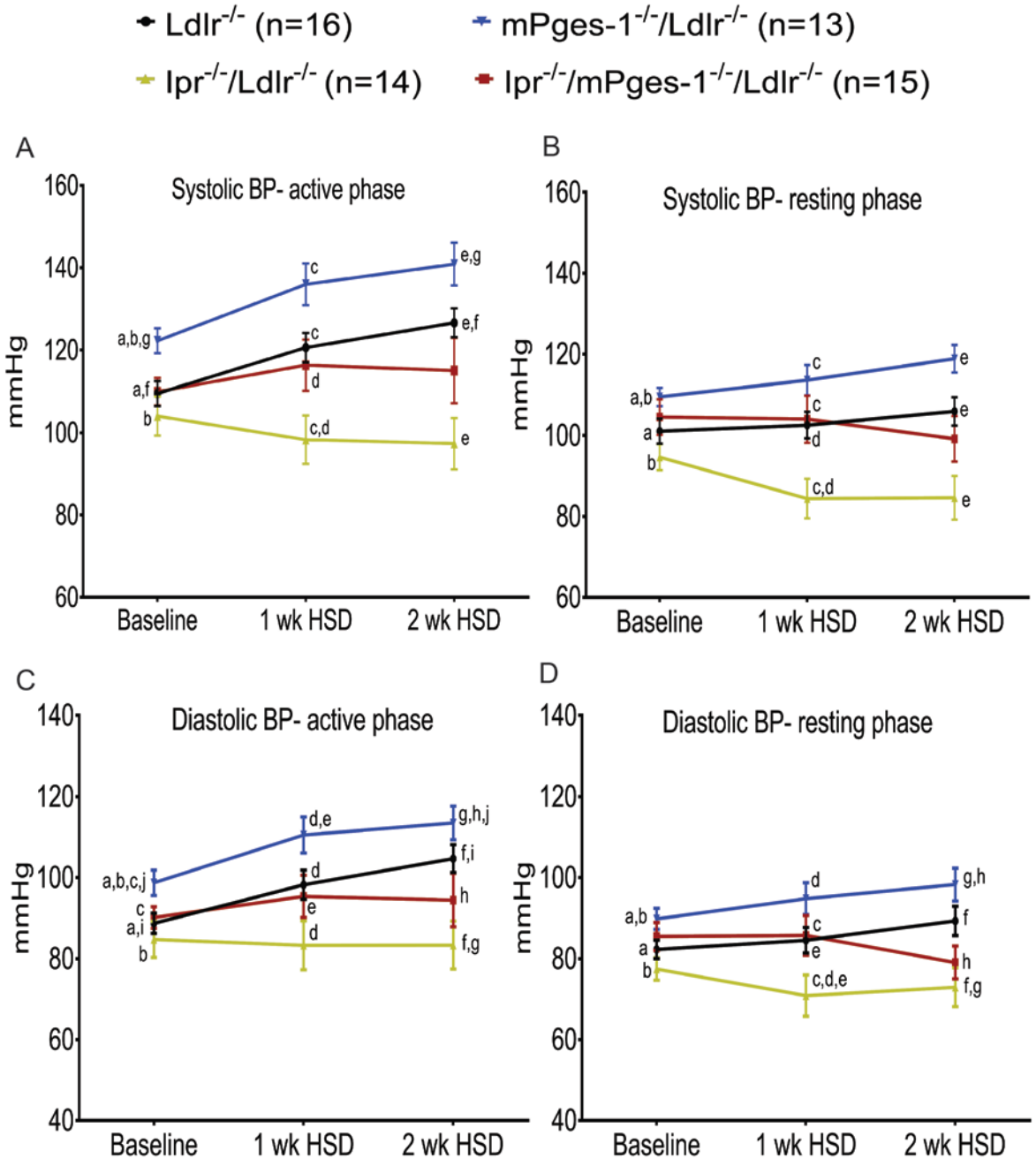

Figure 1. Deletion of Ipr in mPges-1-deficient male hyperlipidemic mice abrogates salt-evoked hypertension. Systolic blood pressures (SBP) in male hyperlipidemic mice and mutants fed a high salt diet (HSD) were measured via telemetry. HSD increased SBPs in Ldlr$^{-/-}$ (Ldlr KO)

mice in a time-dependent pattern, during both the active (night) and resting (day) periods (A-B). Deletion of mPges-1 in $Ldlr^{-/-}$ mice augmented salt-evoked hypertension. By contrast, deletion of prostacyclin receptor (Ipr) restrains salt-evoked hypertension and abrogated hypertensive phenotype in $Ipr^{-/-}$/mPges-$1^{-/-}$/$Ldlr^{-/-}$ mutants. 4-way ANOVA with repeated measures showed a significant effect of Ip, mPges-1, phase and a few of the 2- and 4-way interactions (Ipr:week, week:phase, Ipr:mPges-1:week:phase) on SBP. A posthoc pairwise t-test showed a significant effect on SBP at week 2 in respect to baseline for $Ldlr^{-/-}$ mice. (C-D) Similar trends in DBP responses were observed in all mutants and their littermate controls fed an HSD both in active and resting periods. 4-way ANOVA with repeated measures showed a significant effect of Ipr, week, phase and week:phase interaction on DBP. Pairwise t-test showed significant effect on DBP only at week 2 in respect to baseline for $Ldlr^{-/-}$ mice. Pairwise t-tests were used to test significant differences between $Ldlr^{-/-}$, $Ipr^{-/-}$/mPges-$1^{-/-}$/$Ldlr^{-/-}$, $Ipr^{-/-}$/$Ldlr^{-/-}$ (DKO) and mPges-$1^{-/-}$ /$Ldlr^{-/-}$ mice. Genotypes and feeding periods with the same lower case letter are significantly different (a-j, $p< 0.05$) at baseline, 1 wk HSD or 2 wk HSD. For example, a- baseline SBP (active phase) of mPges-$1^{-/-}$/$Ldlr^{-/-}$ (DKO) was significantly elevated compared with $Ldlr^{-/-}$ and b-$Ipr^{-/-}$/$Ldlr^{-/-}$ mice; f- SBP (active phase) of mPges-$1^{-/-}$/$Ldlr^{-/-}$ mice was significantly elevated at 2 wk HSD compared with baseline. Data are expressed as means ± SEMs. n=13-16 per genotype.

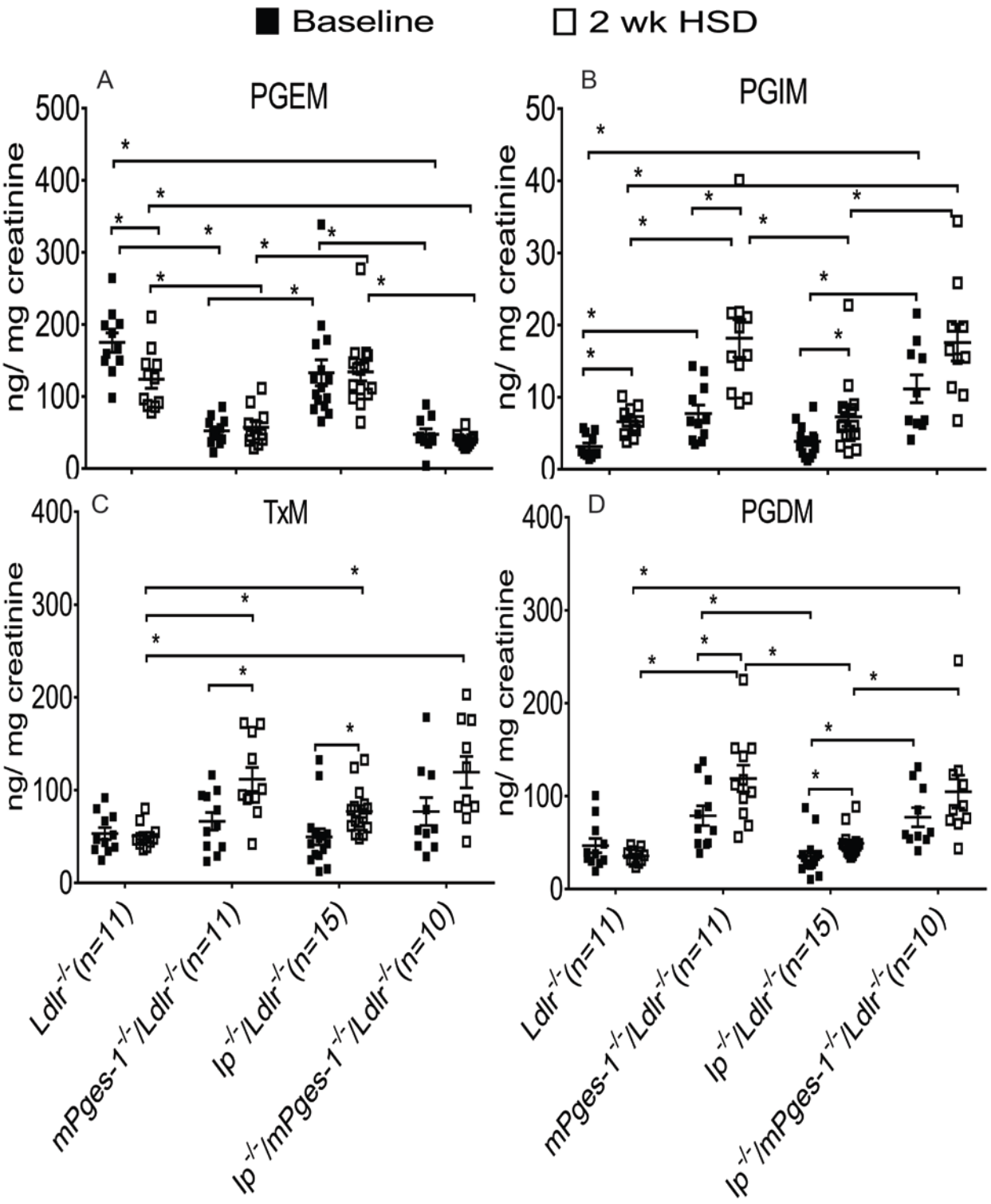

Figure 2. Impact of Ipr and mPges-1 deletion on prostaglandin biosynthesis in male hyperlipidemic mice on a high salt diet. Fasting (9am-4pm) urine samples from $Ldlr^{-/-}$,

mPges-$1^{-/-}$/$Ldlr^{-/-}$, $Ipr^{-/-}$/$Ldlr^{-/-}$ and $Ipr^{-/-}$/mPges-$1^{-/-}$/$Ldlr^{-/-}$ mice were collected before and two weeks after feeding a HSD and prostanoid metabolites were analyzed by liquid chromatography/ mass spectrometry, as described in the Methods. $Ldlr^{-/-}$ mice fed an HSD suppressed PGE_2 but increased PGI_2 biosynthesis as reflected in their urinary PGEM (7-hydroxy-5, 11-diketotetranorprostane-1, 16-dioic acid) (A) and PGIM (2, 3-dinor 6-keto $PGF_{1\alpha}$) (B) metabolites, respectively. Deletion of mPges-1 suppressed PGE_2 but increased PGI_2 biosynthesis in mPges-$1^{-/-}$/$Ldlr^{-/-}$ and $Ipr^{-/-}$/mPges-$1^{-/-}$/$Ldlr^{-/-}$ mice. Deletion of Ipr did not alter PGEM and PGIM levels at baseline but increased PGIM on the HSD. Feeding a HSD also increased urinary 2, 3-dinor TxB_2 (TxM) levels in double knockout mutants (C). After feeding a HSD, urinary PGDM (11, 15-dioxo-9α-hydroxy-2,3,4,5-tetranorprostan-1,20-dioic acid) (D) levels were significantly elevated in the mPges-$1^{-/-}$/$Ldlr^{-/-}$ and $Ipr^{-/-}$/$Ldlr^{-/-}$ mice. 3-way ANOVA showed that urinary PGIM, PGDM and TxM were significantly affected by mPges-1 deletion when mice were fed an HSD. PGEM interacted significantly alone and together with Ipr status and whether the mice were on an HSD. Pairwise t-tests were used to test for significant differences between $Ldlr^{-/-}$, $Ipr^{-/-}$/mPges-$1^{-/-}$/ $Ldlr^{-/-}$, $Ipr^{-/-}$/$Ldlr^{-/-}$ and mPges-$1^{-/-}$/$Ldlr^{-/-}$ mice. Data are expressed as means ± SEMs. *$p< 0.05$; n=10-15 per genotype.

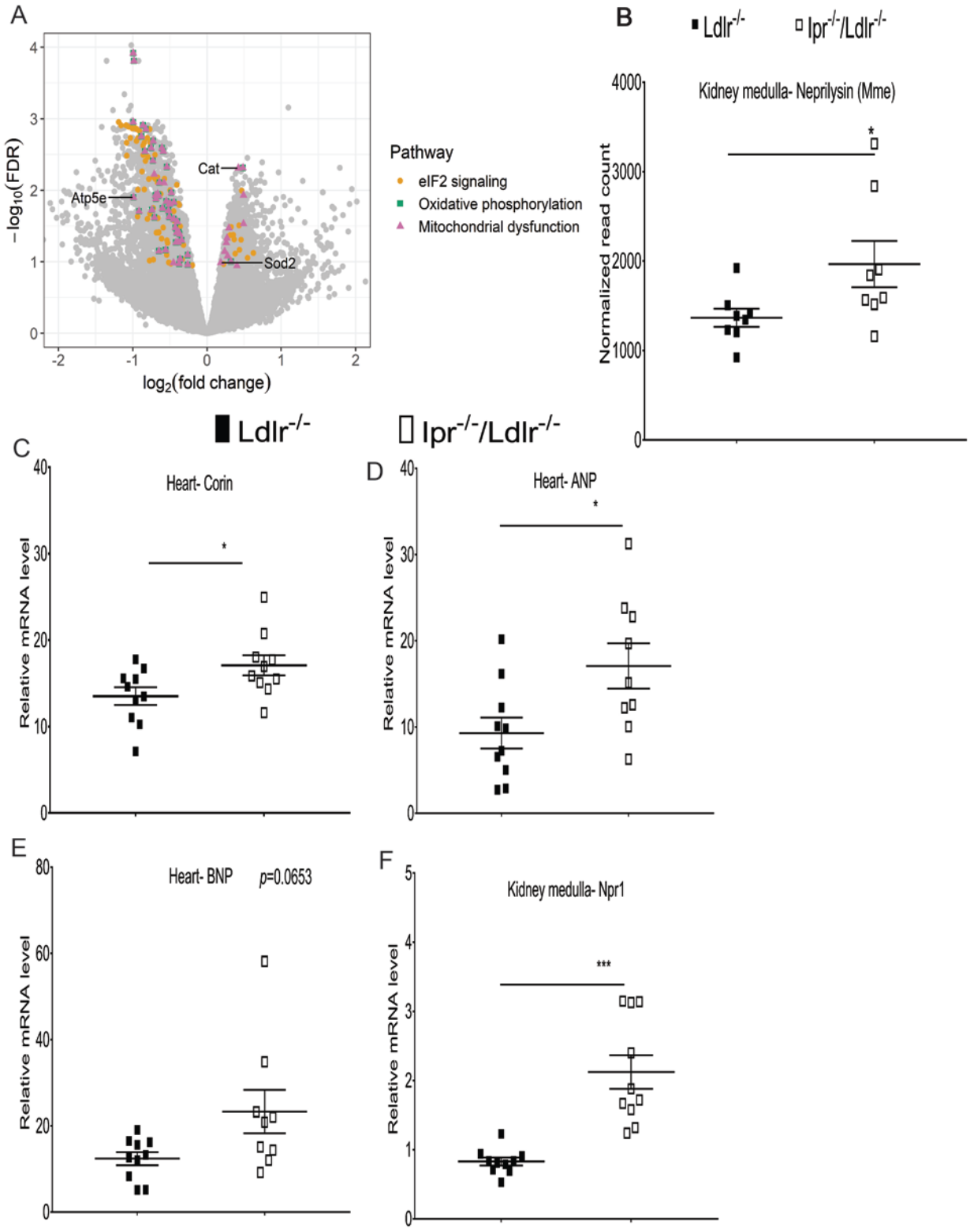
A
Cat
Atp5e
Sod2
−log10(FDR)
log2(fold change)
Pathway
eIF2 signaling
Oxidative phosphorylation
Mitochondrial dysfunction
B
Ldlr-/-
Ipr-/-/Ldlr-/-
Kidney medulla- Neprilysin (Mme)
Normalized read count
C
Heart- Corin
Relative mRNA level
D
Heart- ANP
E
Heart- BNP
p=0.0653
F
Kidney medulla- Npr1

Figure 3. Combined Ipr deletion and salt-evoked hypertension downregulates eIF2, mitochondrial dysfunction and oxidative phosphorylation pathways and activates atrial natriuretic peptide synthesis. RNA samples isolated from kidney medulla of $Ldlr^{-/-}$ and $Ipr^{-/-}$ /$Ldlr^{-/-}$ mice after two weeks on an HSD were used for RNA-Seq. (A) Analysis of signaling pathways. A Volcano plot compares overlap of genes identified in the top three canonical pathways: eIF2 signaling, mitochondrial dysfunction and oxidative phosphorylation. 76 genes in eIF2 signaling pathway were unique. 47 genes were common between mitochondrial dysfunction and oxidative phosphorylation, and 13 genes were unique to mitochondrial dysfunction. Atp5e, Cat and Sod2 are genes validated by RT-qPCR. (B) Neprilysin (Mme) transcript was increased in $Ipr^{-/-}$/$Ldlr^{-/-}$ mice compared with $Ldlr^{-/-}$ mice. (C-F) Real-time PCR was used to measure the expression of corin (ANP-converting enzyme), atrial natriuretic peptide (ANP) and brain natriuretic peptide (BNP) in whole heart and kidney medullary Npr1 (a receptor of ANP). Feeding HSD increased corin and ANP transcripts in heart and Npr1 in kidney medulla of $Ipr^{-/-}$ /$Ldlr^{-/-}$ mice compared with $Ldlr^{-/-}$ mice. BNP gene was not significantly altered between $Ldlr^{-/-}$ and $Ipr^{-/-}$/$Ldlr^{-/-}$ mice. Data are expressed as means ± SEMs (Parametric test, two-tailed, $*p< 0.05$, $***p< 0.001$; n=9-10 per genotype).

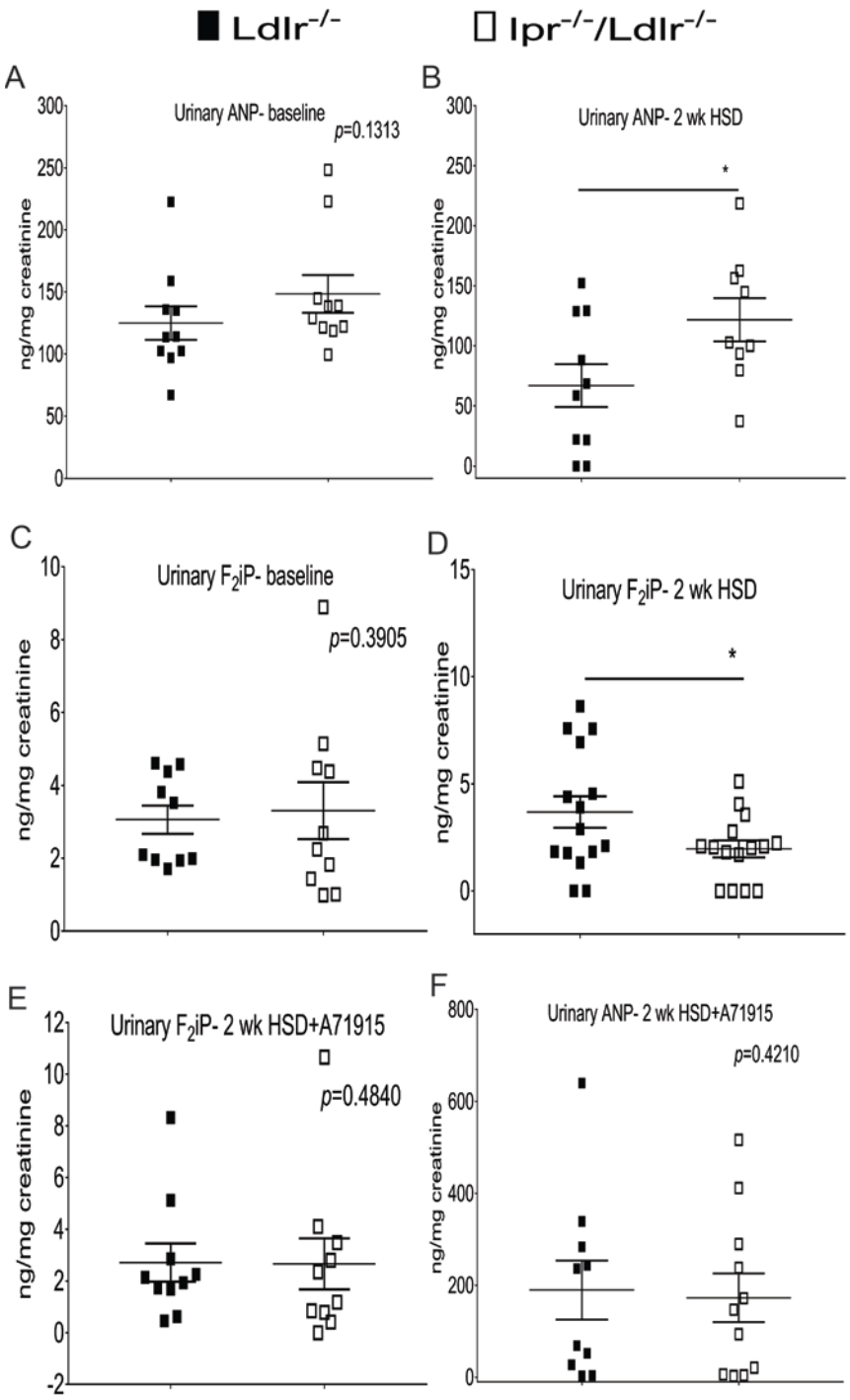
Ldlr-/-
Ipr-/-/Ldlr-/-
A
Urinary ANP- baseline
p=0.1313
ng/mg creatinine
B
Urinary ANP- 2 wk HSD
*
C
Urinary F2iP- baseline
p=0.3905
D
Urinary F2iP- 2 wk HSD
*
E
Urinary F2iP- 2 wk HSD+A71915
p=0.4840
F
Urinary ANP- 2 wk HSD+A71915
p=0.4210

Figure 4. Combined deletion of Ipr and salt-evoked hypertension increases urinary atrial natriuretic peptide and reduces F_2-isoprostanes. Urinary ANP levels at baseline (A) and two weeks after a HSD (B) were measured using an ELISA kit. Urinary ANP levels were elevated in $Ipr^{-/-}/Ldlr^{-/-}$ mice compared with $Ldlr^{-/-}$ mice two weeks after feeding an HSD. An abundant urinary F_2-isoprostane (8,12-*iso*-iPF2α-VI) was analyzed by liquid chromatography/ mass spectrometry as described in the methods. (C- D) The urinary F_2iP was not altered in $Ipr^{-/-}/Ldlr^{-/-}$ mice compared with $Ldlr^{-/-}$ mice at baseline, but the urinary F_2iP in $Ipr^{-/-}/Ldlr^{-/-}$ mice was significantly reduced by two weeks HSD. Treatment with ANP receptor antagonist, A71915 (50µg/Kg BW/day), abrogated the reduction of urinary ANP (E) and urinary F_2iP (F) in $Ipr^{-/-}/Ldlr^{-/-}$ mice. Data are expressed as means ± SEMs (Parametric test, Welch's correction, one-tailed, $*p< 0.05$; n=9-15 per genotype). We used a one-tailed test for urinary F_2iP and ANP because both mediators had been already shown to restrain oxidative stress in the vasculature.

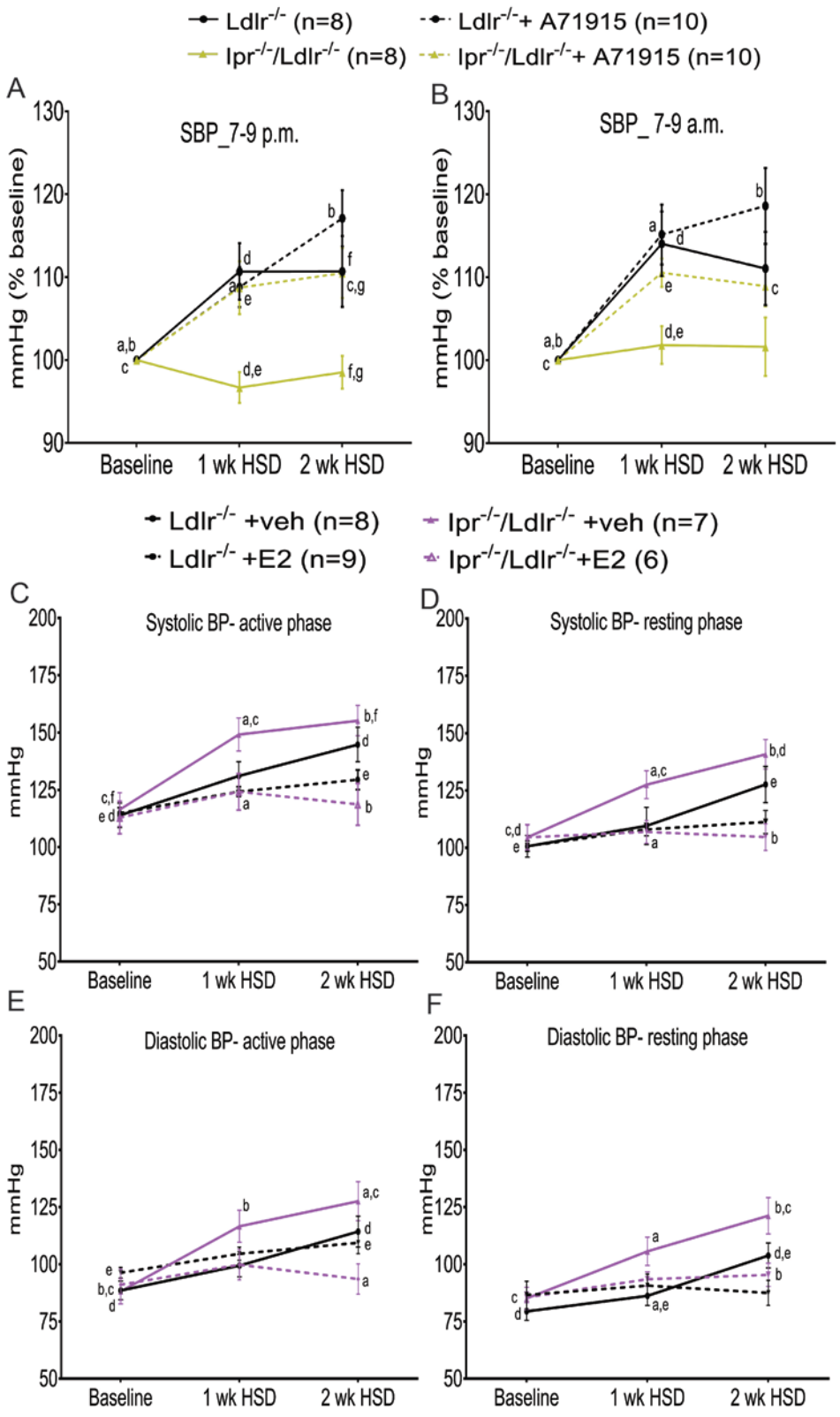
Ldlr-/- (n=8)
Ldlr-/-+ A71915 (n=10)
Ipr-/-/Ldlr-/- (n=8)
Ipr-/-/Ldlr-/-+ A71915 (n=10)
A
SBP_7-9 p.m.
mmHg (% baseline)
130
120
110
100
90
Baseline
1 wk HSD
2 wk HSD
B
SBP_ 7-9 a.m.
Ldlr-/- +veh (n=8)
Ldlr-/- +E2 (n=9)
Ipr-/-/Ldlr-/- +veh (n=7)
Ipr-/-/Ldlr-/-+E2 (6)
C
Systolic BP- active phase
mmHg
200
175
150
125
100
75
50
D
Systolic BP- resting phase
E
Diastolic BP- active phase
F
Diastolic BP- resting phase

Figure 5. The atrial natriuretic peptide receptor antagonist (A71915) and estrogen mediate salt-evoked BP responses in Ipr-deficient male and female hyperlipidemic mice, respectively. The ANP antagonist (A71915) rescues hypotension in $Ip^{-/-}$/$Ldlr^{-/-}$ mice fed a HSD. Systolic blood pressures (SBP, A- active phase, B- resting phase) of male mice with and without mini-pumps were measured using a tail-cuff system before, one and two weeks after feeding a HSD in conjunction with and without ANP inhibition via A71915 infusion (50µg/Kg BW/day). To compare the effect of Ipr deletion and A71915 administration, genotype and feeding time with the same lower case letter are significantly different (a- g, $p< 0.05$) at 1 wk HSD or 2 wk HSD. For example, a- SBP (active phase) of $Ipr^{-/-}$/$Ldlr^{-/-}$ mice was significantly elevated at 1 wk HSD and b- 2 wk HSD compared with baseline; d- SBP (active phase) of $Ldlr^{-/-}$ mice was significantly elevated compared with $Ipr^{-/-}$/$Ldlr^{-/-}$ mice at 1 wk HSD; etc. Data are expressed as means ± SEMs. n=8-10 per group. (C-F) Salt loading increased BP in ovariectomized female $Ldlr^{-/-}$ and $Ipr^{-/-}$/$Ldlr^{-/-}$ mice. Estradiol (E2) replacement restrained the BP responses. To compare the effect of Ipr deletion and E2 administration, genotype and/ or feeding time with the same lower case letter are significantly different (a- f, $p< 0.05$) at 1 wk HSD or 2 wk HSD. For example, a- SBP (active phase) of Ipr/Ldlr DKO+veh was significantly higher compared with $Ipr^{-/-}$/$Ldlr^{-/-}$ +E2 at 1 wk HSD and b- 2 wk HSD; c- SBP (active phase) of $Ipr^{-/-}$/$Ldlr^{-/-}$ +veh was significantly higher at 1 wk HSD compared with baseline; etc. Data are expressed as means ± SEMs. n=6-9 per group.

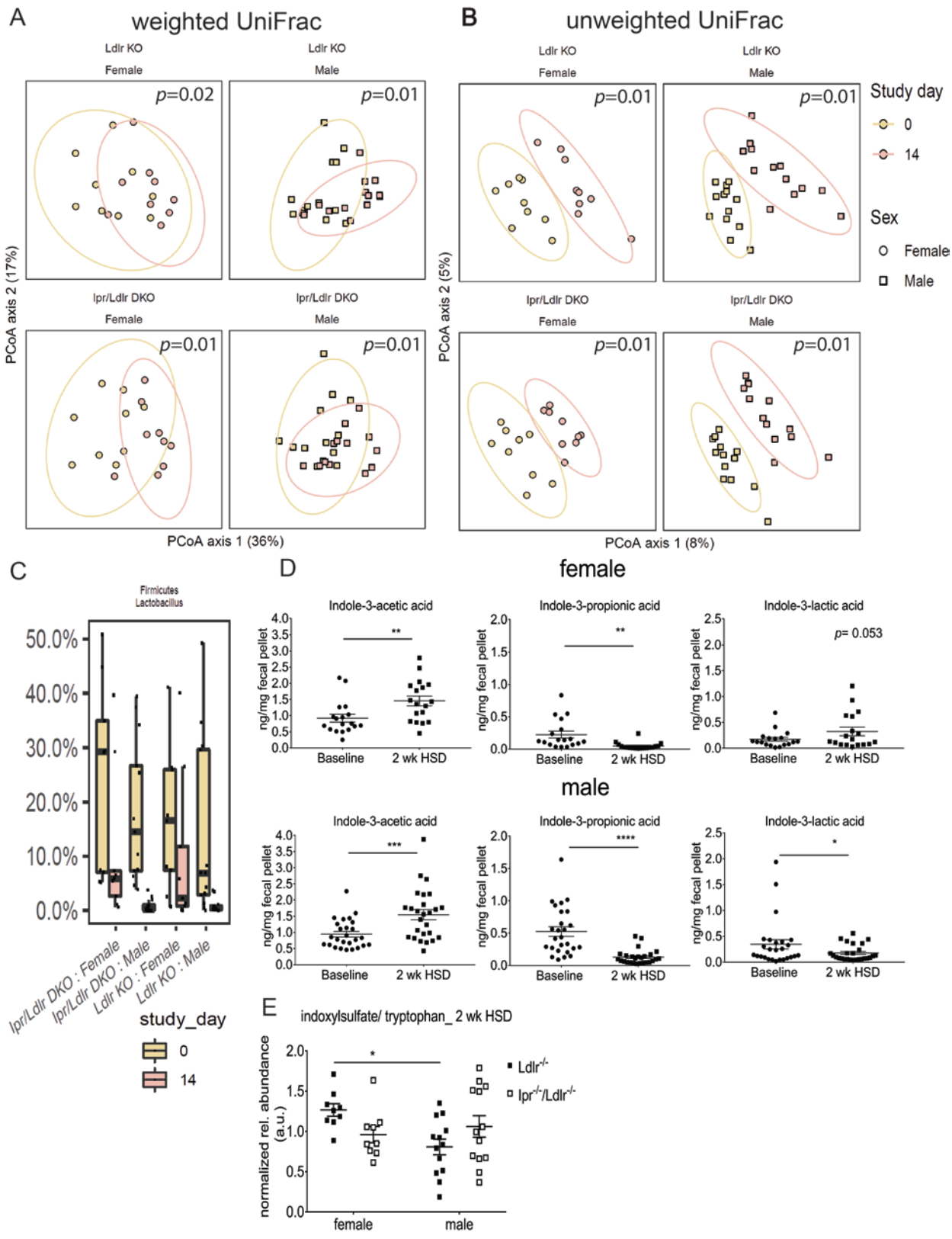
A
weighted UniFrac
Ldlr KO
Female
Ldlr KO
Male
Ipr/Ldlr DKO
Female
Ipr/Ldlr DKO
Male
p=0.02
p=0.01
p=0.01
p=0.01
PCoA axis 2 (17%)
PCoA axis 1 (36%)
B
unweighted UniFrac
Ldlr KO
Female
Ldlr KO
Male
Ipr/Ldlr DKO
Female
Ipr/Ldlr DKO
Male
p=0.01
p=0.01
p=0.01
p=0.01
PCoA axis 2 (5%)
PCoA axis 1 (8%)
Study day
0
14
Sex
Female
Male
C
Firmicutes
Lactobacillus
50.0%
40.0%
30.0%
20.0%
10.0%
0.0%
Ipr/Ldlr DKO : Female
Ipr/Ldlr DKO : Male
Ldlr KO : Female
Ldlr KO : Male
study_day
0
14
D
female
Indole-3-acetic acid
Indole-3-propionic acid
Indole-3-lactic acid
p= 0.053
ng/mg fecal pellet
Baseline
2 wk HSD
male
Indole-3-acetic acid
Indole-3-propionic acid
Indole-3-lactic acid
E
indoxylsulfate/ tryptophan_ 2 wk HSD
normalized rel. abundance (a.u.)
female
male
Ldlr-/-
Ipr-/-/Ldlr-/-

Figure 6. HSD alters gut microbiota composition in a sex-dependent manner. Fecal pellets were collected from singly housed mice at baseline (day 0) and 2 weeks (day 14) after being fed a HSD. Bacterial DNA was extracted and analyzed by 16S rRNA gene sequencing. Regardless of sex or genotypes- Ldlr-/- (Ldlr KO) vs $Ipr^{-/-}/Ldlr^{-/-}$ (Ipr/Ldlr DKO) mice), β-diversity of the gut microbiota was significantly different between day 0 and day 14 as assessed by weighted UniFrac (A) and unweighted UniFrac (B). (C) Relative abundance of *Lactobacillus* was significantly reduced in male $Ldlr^{-/-}$ mice ($p= 1.2x10^{-3}$) and $Ipr^{-/-}/Ldlr^{-/-}$ mice ($p= 2.5x10^{-4}$) mice compared to female mice. (D) Fecal indole metabolites were analyzed by HPLC-MS/MS. HSD significantly increased indole-3-acetic acid in both female and male mice, whereas indole-3-propionic acid decreased. Indole-3-lactic acid was significantly reduced in male mice only. As HSD reduces the abundance of *Lactobacillus*, we performed one-tailed test for fecal indole metabolites. Data are expressed as means ± SEMs (Parametric test, paired, one-tailed, $*p< 0.05$, $**p< 0.01$, $***p< 0.001$; female n= 18, male n= 26 male per genotype). (E) Plasma levels of indoxyl sulfate/ tryptophan was significantly reduced in male $Ldlr^{-/-}$ mice compared with female $Ldlr^{-/-}$ mice after 2 weeks of HSD. Two-way ANOVA showed a significant effect of sex on plasma levels of indoxylsulfate/ tryptophan in $Ldlr^{-/-}$ mice. Sidak's multiple comparison tests were used to test significant differences between sexes. Data are expressed as means ± SEMs, $*p< 0.05$, female n= 9, male n= 13 per genotype).

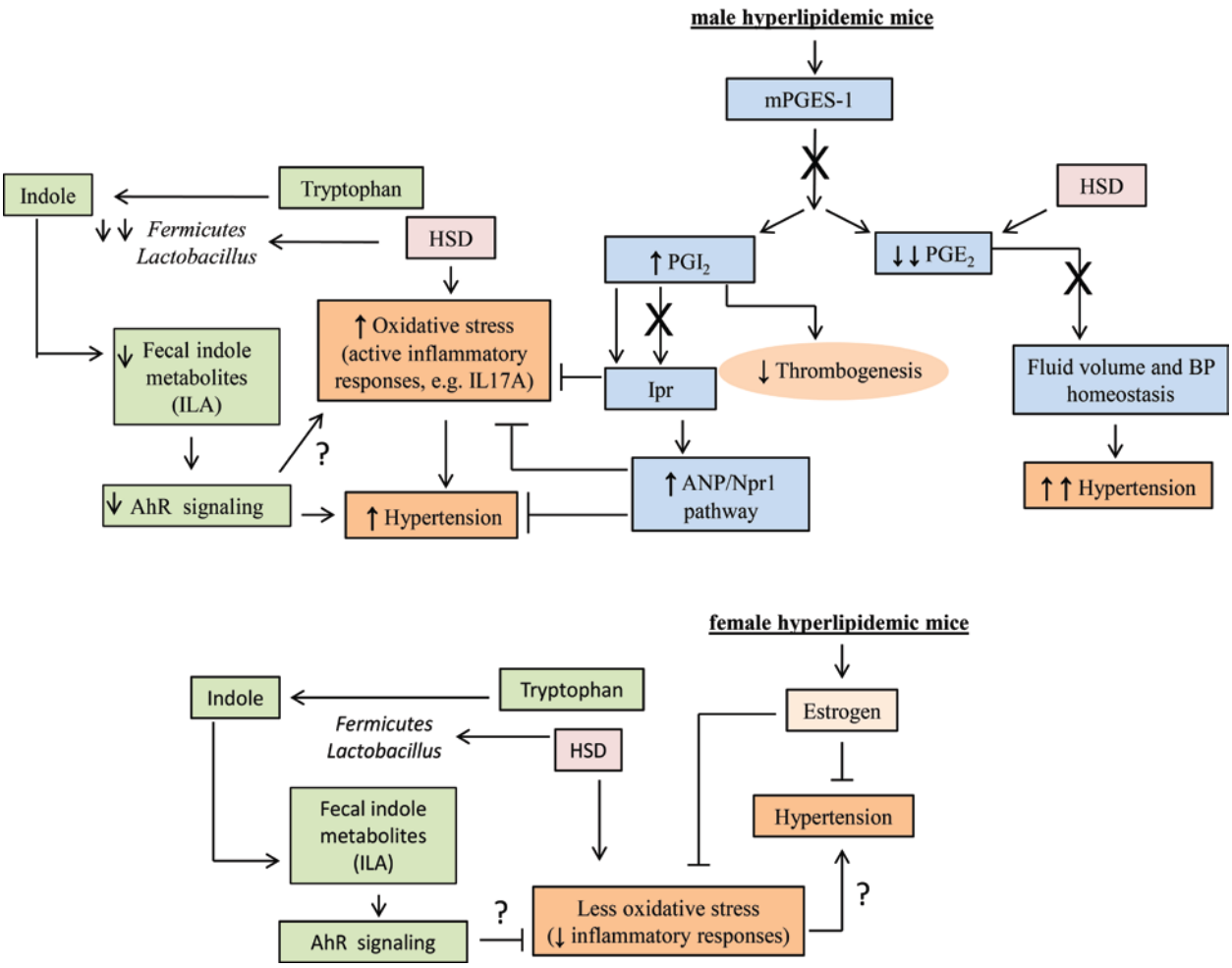

Figure 7. Schema depicting the effect of a high salt diet in prostaglandin I_2 receptor deficient male and female mice. Deletion of mPges-1 suppresses PGE_2 biosynthesis while increasing PGI_2, which contributes to the attenuation of thrombogenesis in hyperlipidemic mice. However, salt loading suppresses PGE_2 biosynthesis and increases BP responses. Both PGI_2 and ANP are vasodilators and restrain oxidative stress induced by a HSD. Deletion of Ipr resulted in the compensatory increase in ANP/ Npr1 signaling and reduced mitochondrial oxidative stress and BP responses. In female hyperlipidemic mice, estrogen protects $Ldlr^{-/-}$ and $Ipr^{-/-}/Ldlr^{-/-}$ mice from salt-evoked hypertension. HSD suppresses the abundance of *Lactobacillus* in male mice and reduces levels of indole metabolites such as indole-3-lactic acid. ILA binds AhR and

activates signaling pathways that might restrain oxidative stress and hypertension. mPGES-1 indicates microsomal prostaglandin E synthase 1; PGE_2, prostaglandin E_2; PGI_2, prostacyclin, Ipr, I prostanoid receptor; ANP- atrial natriuretic peptide; Npr1, receptor of ANP; BP, blood pressure; X, inhibition or deletion of enzyme; ⊣, restrain; HSD, high salt diet; AhR, aryl hydrocarbon receptor; ILA, indole-3-lactic acid.

Reference

1. Samuelsson, B., Morgenstern, R., and Jakobsson, P.J. 2007. Membrane prostaglandin E synthase-1: a novel therapeutic target. *Pharmacol Rev* 59:207-224.
2. Koeberle, A., and Werz, O. 2015. Perspective of microsomal prostaglandin E2 synthase-1 as drug target in inflammation-related disorders. *Biochem Pharmacol* 98:1-15.
3. Cheng, Y., Wang, M., Yu, Y., Lawson, J., Funk, C.D., and Fitzgerald, G.A. 2006. Cyclooxygenases, microsomal prostaglandin E synthase-1, and cardiovascular function. *J Clin Invest* 116:1391-1399.
4. Grosser, T., Woolf, C.J., and FitzGerald, G.A. 2017. Time for nonaddictive relief of pain. *Science* 355:1026-1027.
5. FitzGerald, G.A. 2003. COX-2 and beyond: Approaches to prostaglandin inhibition in human disease. *Nat Rev Drug Discov* 2:879-890.
6. Armstrong, E.P., and Malone, D.C. 2003. The impact of nonsteroidal anti-inflammatory drugs on blood pressure, with an emphasis on newer agents. *Clin Ther* 25:1-18.
7. Johnson, A.G., Nguyen, T.V., and Day, R.O. 1994. Do nonsteroidal anti-inflammatory drugs affect blood pressure? A meta-analysis. *Ann Intern Med* 121:289-300.
8. Pope, J.E., Anderson, J.J., and Felson, D.T. 1993. A meta-analysis of the effects of nonsteroidal anti-inflammatory drugs on blood pressure. *Arch Intern Med* 153:477-484.
9. Tang, S.Y., Monslow, J., G, R.G., Todd, L., Pawelzik, S.C., Chen, L., Lawson, J., Pure, E., and FitzGerald, G.A. 2016. Cardiovascular Consequences of Prostanoid I Receptor Deletion in Microsomal Prostaglandin E Synthase-1-Deficient Hyperlipidemic Mice. *Circulation* 134:328-338.
10. von Eiff, A.W., Gogolin, E., Jacobs, U., and Neus, H. 1986. Ambulatory blood pressure in children followed for 3 years. Influence of sex and family history of hypertension. *Clin Exp Hypertens A* 8:577-581.
11. Myers, J., and Morgan, T. 1983. The effect of sodium intake on the blood pressure related to age and sex. *Clin Exp Hypertens A* 5:99-118.
12. Dahl, L.K., Knudsen, K.D., Ohanian, E.V., Muirhead, M., and Tuthill, R. 1975. Role of the gonads in hypertension-prone rats. *J Exp Med* 142:748-759.
13. Haywood, J.R., and Hinojosa-Laborde, C. 1997. Sexual dimorphism of sodium-sensitive renal-wrap hypertension. *Hypertension* 30:667-671.
14. Stock, J.L., Shinjo, K., Burkhardt, J., Roach, M., Taniguchi, K., Ishikawa, T., Kim, H.S., Flannery, P.J., Coffman, T.M., McNeish, J.D., et al. 2001. The prostaglandin E2 EP1 receptor mediates pain perception and regulates blood pressure. *J Clin Invest* 107:325-331.
15. Bartolomaeus, H., Marko, L., Wilck, N., Luft, F.C., Forslund, S.K., and Muller, D.N. 2019. Precarious Symbiosis Between Host and Microbiome in Cardiovascular Health. *Hypertension* 73:926-935.

16. Madhur, M.S., Elijovich, F., Alexander, M.R., Pitzer, A., Ishimwe, J., Van Beusecum, J.P., Patrick, D.M., Smart, C.D., Kleyman, T.R., Kingery, J., et al. 2021. Hypertension: Do Inflammation and Immunity Hold the Key to Solving this Epidemic? *Circ Res* 128:908-933.
17. Wenzel, U.O., Bode, M., Kohl, J., and Ehmke, H. 2017. A pathogenic role of complement in arterial hypertension and hypertensive end organ damage. *Am J Physiol Heart Circ Physiol* 312:H349-H354.
18. Li, J., Yang, X., Zhou, X., and Cai, J. 2021. The Role and Mechanism of Intestinal Flora in Blood Pressure Regulation and Hypertension Development. *Antioxid Redox Signal* 34:811-830.
19. Palmu, J., Salosensaari, A., Havulinna, A.S., Cheng, S., Inouye, M., Jain, M., Salido, R.A., Sanders, K., Brennan, C., Humphrey, G.C., et al. 2020. Association Between the Gut Microbiota and Blood Pressure in a Population Cohort of 6953 Individuals. *J Am Heart Assoc* 9:e016641.
20. Steinhelper, M.E., Cochrane, K.L., and Field, L.J. 1990. Hypotension in transgenic mice expressing atrial natriuretic factor fusion genes. *Hypertension* 16:301-307.
21. Melo, L.G., Veress, A.T., Ackermann, U., Steinhelper, M.E., Pang, S.C., Tse, Y., and Sonnenberg, H. 1999. Chronic regulation of arterial blood pressure in ANP transgenic and knockout mice: role of cardiovascular sympathetic tone. *Cardiovasc Res* 43:437-444.
22. Reilly, M.P., Pratico, D., Delanty, N., DiMinno, G., Tremoli, E., Rader, D., Kapoor, S., Rokach, J., Lawson, J., and FitzGerald, G.A. 1998. Increased formation of distinct F2 isoprostanes in hypercholesterolemia. *Circulation* 98:2822-2828.
23. Egan, K.M., Lawson, J.A., Fries, S., Koller, B., Rader, D.J., Smyth, E.M., and Fitzgerald, G.A. 2004. COX-2-derived prostacyclin confers atheroprotection on female mice. *Science* 306:1954-1957.
24. Bayorh, M.A., Ganafa, A.A., Socci, R.R., Silvestrov, N., and Abukhalaf, I.K. 2004. The role of oxidative stress in salt-induced hypertension. *Am J Hypertens* 17:31-36.
25. Dornas, W.C., Cardoso, L.M., Silva, M., Machado, N.L., Chianca, D.A., Jr., Alzamora, A.C., Lima, W.G., Lagente, V., and Silva, M.E. 2017. Oxidative stress causes hypertension and activation of nuclear factor-kappaB after high-fructose and salt treatments. *Sci Rep* 7:46051.
26. von Geldern, T.W., Budzik, G.P., Dillon, T.P., Holleman, W.H., Holst, M.A., Kiso, Y., Novosad, E.I., Opgenorth, T.J., Rockway, T.W., Thomas, A.M., et al. 1990. Atrial natriuretic peptide antagonists: biological evaluation and structural correlations. *Mol Pharmacol* 38:771-778.
27. Park, B.M., Gao, S., Cha, S.A., and Kim, S.H. 2015. Attenuation of renovascular hypertension by cyclooxygenase-2 inhibitor partly through ANP release. *Peptides* 69:1-8.
28. Delporte, C., Winand, J., Poloczek, P., Von Geldern, T., and Christophe, J. 1992. Discovery of a potent atrial natriuretic peptide antagonist for ANPA receptors in the human neuroblastoma NB-OK-1 cell line. *Eur J Pharmacol* 224:183-188.
29. Romero, M., Caniffi, C., Bouchet, G., Costa, M.A., Elesgaray, R., Arranz, C., and Tomat, A.L. 2015. Chronic treatment with atrial natriuretic peptide in spontaneously hypertensive rats: beneficial renal effects and sex differences. *PLoS One* 10:e0120362.
30. Grosser, T., Ricciotti, E., and FitzGerald, G.A. 2017. The Cardiovascular Pharmacology of Nonsteroidal Anti-Inflammatory Drugs. *Trends Pharmacol Sci* 38:733-748.
31. Watanabe, H., Katoh, T., Eiro, M., Iwamoto, M., Ushikubi, F., Narumiya, S., and Watanabe, T. 2005. Effects of salt loading on blood pressure in mice lacking the prostanoid receptor gene. *Circ J* 69:124-126.
32. Francois, H., Athirakul, K., Howell, D., Dash, R., Mao, L., Kim, H.S., Rockman, H.A., Fitzgerald, G.A., Koller, B.H., and Coffman, T.M. 2005. Prostacyclin protects against elevated blood pressure and cardiac fibrosis. *Cell Metab* 2:201-207.
33. Wang, M., Zukas, A.M., Hui, Y., Ricciotti, E., Pure, E., and FitzGerald, G.A. 2006. Deletion of microsomal prostaglandin E synthase-1 augments prostacyclin and retards atherogenesis. *Proc Natl Acad Sci U S A* 103:14507-14512.

34. Wang, M., and FitzGerald, G.A. 2010. Cardiovascular biology of microsomal prostaglandin E synthase-1. *Trends Cardiovasc Med* 20:189-195.
35. Jin, Y., Smith, C.L., Hu, L., Campanale, K.M., Stoltz, R., Huffman, L.G., Jr., McNearney, T.A., Yang, X.Y., Ackermann, B.L., Dean, R., et al. 2016. Pharmacodynamic comparison of LY3023703, a novel microsomal prostaglandin e synthase 1 inhibitor, with celecoxib. *Clin Pharmacol Ther* 99:274-284.
36. Kennedy, C.R., Zhang, Y., Brandon, S., Guan, Y., Coffee, K., Funk, C.D., Magnuson, M.A., Oates, J.A., Breyer, M.D., and Breyer, R.M. 1999. Salt-sensitive hypertension and reduced fertility in mice lacking the prostaglandin EP2 receptor. *Nat Med* 5:217-220.
37. Harris, R.C., and Breyer, M.D. 2006. Update on cyclooxygenase-2 inhibitors. *Clin J Am Soc Nephrol* 1:236-245.
38. Smolenski, A. 2012. Novel roles of cAMP/cGMP-dependent signaling in platelets. *J Thromb Haemost* 10:167-176.
39. John, S.W., Krege, J.H., Oliver, P.M., Hagaman, J.R., Hodgin, J.B., Pang, S.C., Flynn, T.G., and Smithies, O. 1995. Genetic decreases in atrial natriuretic peptide and salt-sensitive hypertension. *Science* 267:679-681.
40. Laskowski, A., Woodman, O.L., Cao, A.H., Drummond, G.R., Marshall, T., Kaye, D.M., and Ritchie, R.H. 2006. Antioxidant actions contribute to the antihypertrophic effects of atrial natriuretic peptide in neonatal rat cardiomyocytes. *Cardiovasc Res* 72:112-123.
41. Pandey, K.N. 2011. Guanylyl cyclase / atrial natriuretic peptide receptor-A: role in the pathophysiology of cardiovascular regulation. *Can J Physiol Pharmacol* 89:557-573.
42. Ichiki, T., and Burnett, J.C., Jr. 2017. Atrial Natriuretic Peptide- Old But New Therapeutic in Cardiovascular Diseases. *Circ J* 81:913-919.
43. Mendelsohn, M.E. 2002. Protective effects of estrogen on the cardiovascular system. *Am J Cardiol* 89:12E-17E; discussion 17E-18E.
44. Chang, W.C., Nakao, J., Neichi, T., Orimo, H., and Murota, S. 1981. Effects of estradiol on the metabolism of arachidonic acid by aortas and platelets in rats. *Biochim Biophys Acta* 664:291-297.
45. Chang, W.C., Nakao, J., Orimo, H., and Murota, S. 1980. Stimulation of prostacyclin biosynthetic activity by estradiol in rat aortic smooth muscle cells in culture. *Biochim Biophys Acta* 619:107-118.
46. Mikkola, T., Turunen, P., Avela, K., Orpana, A., Viinikka, L., and Ylikorkala, O. 1995. 17 beta-estradiol stimulates prostacyclin, but not endothelin-1, production in human vascular endothelial cells. *J Clin Endocrinol Metab* 80:1832-1836.
47. Wilck, N., Matus, M.G., Kearney, S.M., Olesen, S.W., Forslund, K., Bartolomaeus, H., Haase, S., Mahler, A., Balogh, A., Marko, L., et al. 2017. Salt-responsive gut commensal modulates TH17 axis and disease. *Nature* 551:585-589.
48. Itani, H.A., McMaster, W.G., Jr., Saleh, M.A., Nazarewicz, R.R., Mikolajczyk, T.P., Kaszuba, A.M., Konior, A., Prejbisz, A., Januszewicz, A., Norlander, A.E., et al. 2016. Activation of Human T Cells in Hypertension: Studies of Humanized Mice and Hypertensive Humans. *Hypertension* 68:123-132.
49. Amador, C.A., Barrientos, V., Pena, J., Herrada, A.A., Gonzalez, M., Valdes, S., Carrasco, L., Alzamora, R., Figueroa, F., Kalergis, A.M., et al. 2014. Spironolactone decreases DOCA-salt-induced organ damage by blocking the activation of T helper 17 and the downregulation of regulatory T lymphocytes. *Hypertension* 63:797-803.
50. Madhur, M.S., Lob, H.E., McCann, L.A., Iwakura, Y., Blinder, Y., Guzik, T.J., and Harrison, D.G. 2010. Interleukin 17 promotes angiotensin II-induced hypertension and vascular dysfunction. *Hypertension* 55:500-507.

51. Barhoumi, T., Kasal, D.A., Li, M.W., Shbat, L., Laurant, P., Neves, M.F., Paradis, P., and Schiffrin, E.L. 2011. T regulatory lymphocytes prevent angiotensin II-induced hypertension and vascular injury. *Hypertension* 57:469-476.
52. Norlander, A.E., Bloodworth, M.H., Toki, S., Zhang, J., Zhou, W., Boyd, K., Polosukhin, V.V., Cephus, J.Y., Ceneviva, Z.J., Gandhi, V.D., et al. 2021. Prostaglandin I2 signaling licenses Treg suppressive function and prevents pathogenic reprogramming. *J Clin Invest* 131.
53. Miranda, P.M., De Palma, G., Serkis, V., Lu, J., Louis-Auguste, M.P., McCarville, J.L., Verdu, E.F., Collins, S.M., and Bercik, P. 2018. High salt diet exacerbates colitis in mice by decreasing Lactobacillus levels and butyrate production. *Microbiome* 6:57.
54. Zelante, T., Iannitti, R.G., Cunha, C., De Luca, A., Giovannini, G., Pieraccini, G., Zecchi, R., D'Angelo, C., Massi-Benedetti, C., Fallarino, F., et al. 2013. Tryptophan catabolites from microbiota engage aryl hydrocarbon receptor and balance mucosal reactivity via interleukin-22. *Immunity* 39:372-385.
55. Cervantes-Barragan, L., Chai, J.N., Tianero, M.D., Di Luccia, B., Ahern, P.P., Merriman, J., Cortez, V.S., Caparon, M.G., Donia, M.S., Gilfillan, S., et al. 2017. Lactobacillus reuteri induces gut intraepithelial CD4(+)CD8alphaalpha(+) T cells. *Science* 357:806-810.
56. Rothhammer, V., and Quintana, F.J. 2019. The aryl hydrocarbon receptor: an environmental sensor integrating immune responses in health and disease. *Nat Rev Immunol* 19:184-197.
57. Descamps, H.C., Herrmann, B., Wiredu, D., and Thaiss, C.A. 2019. The path toward using microbial metabolites as therapies. *EBioMedicine* 44:747-754.